Bull Eng Geol Environ
DOI 10.1007/s10064-010-0322-y

ORIGINAL PAPER

The dynamics of coastal landslides: insights from laboratory experiments and theoretical analyses

Paolo Mazzanti · Fabio Vittorio De Blasio

Received: 2 November 2009 / Accepted: 31 July 2010

Abstract Laboratory experiments have been carried out to study the dynamics of landslides commencing subaerially and ending inside a water basin. A comparison between experiments with and without water shows differences in the final deposits. In the subaqueous experiments the grains did not spread out from the mass in the same way as in the subaerial movement. It is suggested that air can be trapped inside the mass which, released during the final stage of the underwater mass propagation, modifies the buoyancy forces. Other effects observed during the air to water transition include the "jumping" and "tilting" of grains. It is concluded that the air to water transition plays a key role in the dynamics of combined subaerial/subaqueous landslides. The information obtained from the experiments may also be useful in the consideration of tsunami generation and the sedimentological analyses of landslide deposits.

Keywords Coastal landslides · Landslides dynamics · Granular flows · Jumping · Air ejection · Water impact

Résumé Des expériences de laboratoire ont été réalisées pour étudier l'évolution de glissements de terrain générés à l'air libre et se terminant dans l'eau. Une comparaison entre des expériences avec ou sans eau montre des différences dans les dépôts finaux. Dans les expériences en milieu aqueux les particules ne s'étalent pas de la même façon que dans les expériences en milieu aérien. Il est suggéré que l'air peut être piégé à l'intérieur de la masse de terrain ce qui, une fois cette masse libérée pendant la phase finale de la propagation sous l'eau, modifie les forces de déjaugeage. D'autres effets observés, durant la phase de transition dans la propagation dans l'air puis dans l'eau, concernent la «saltation» et le «basculement» des particules. Il est conclu que la phase de transition de la propagation dans l'air puis dans l'eau joue un rôle clé dans la dynamique des glissements de terrain sub-aériens/subaqueux. Les informations obtenues à partir des expériences peuvent aussi être utiles dans l'étude de la génération de tsunamis et l'analyse sédimentologique des dépôts de matériaux glissés.

Mots clés Glissements côtiers · Dynamique des glissements de terrain · Ecoulements granulaires · Saltation · Expulsion d'air · Rôle de l'eau

P. Mazzanti (✉) · F. V. De Blasio
NHAZCA S.r.l., spin-off "Sapienza" Università di Roma,
Via Cori snc, 00177 Rome, Italy
e-mail: paolo.mazzanti@uniroma1.it

P. Mazzanti
Dipartimento di Scienze della Terra,
"Sapienza" Università di Roma,
P.le Aldo Moro 5, 00185 Rome, Italy

F. V. De Blasio
Department of Geosciences,
University of Oslo,
P.O. Box 1047 Blindern, 0316 Oslo, Norway

Introduction

Landslides and gravitational mass flows are very common, taking place both in the subaerial and subaqueous environments. Landslides often interact with human activities and represent a threat to settlements and buildings. Furthermore, in the case of landslides interacting with the hydrosphere, there is an additional risk, represented by induced tsunami, that must be taken into account in urban

Published online: 22 September 2010

planning and in designing mitigation measures. This paper concentrates on coastal landslides, i.e. landslides starting subaerially and continuing underwater. They are very complex phenomena as they combine features of subaerial and subaqueous mass movements and the air to water transition. The first step to improving knowledge of these complex events is represented by small scale laboratory experiments.

Although mudflows and cohesive debris flows may also enter water reservoirs, this study considers only dry granular flows. Several experimental studies with granular flows have been undertaken in order to better understand the dynamics of landslides and debris flows. Flumes ranging from 1 m to more than 100 m (Iverson et al. 1992) have been employed to investigate the behaviour of subaerial gravity driven flows (see at Iverson (1997) and Pudasaini and Hutter (2007) for an extensive review). Kuenen and Migliorini (1950) and Hampton (1972) were among the first to perform laboratory flume experiments for subaqueous mass flows, mainly looking at sedimentation processes and turbidity currents. In more recent years the interest in this field has significantly increased, partly with the involvement of the oil industry, and has resulted in numerous experiments (Talling et al. 2002; Marr et al. 2001; Ilstad et al. 2004; Felix and Peakall 2006 among the others).

A comparison between the results inferred from subaerial and subaqueous gravity flows highlights a series of important differences. For example, it has been found that subaqueous debris flows may hydroplane, thus enhancing enormously their run-out distance compared with subaerial debris flows. Moreover, subaerial debris flows exhibit a different effect in the remobilisation of antecedent deposits at the base. Therefore, some specific experiments have recently been performed with the aim of investigating such differences and better understanding the physical mechanisms which control these events. Papers by Mohrig et al. (1999) and Breien et al. (2007) summarize the results of a series of experiments carried out at the St. Anthony Falls Laboratory (SAFL) at the University of Minnesota.

Although there have been a number of experiments on sand–clay mixtures in various proportions to investigate cohesive debris flows, fewer experiments have addressed granular flows in water. This is particularly true for granular flows which start subaerially, plunge into water and propagate themselves underwater. To the authors' knowledge, only preliminary experiments have been performed by Naruse and Masuda at Kyoto University (personal communication) in order to analyse the transformation of the flow during the air to water transition and the subsequent subaqueous path. They observed that a transformation from debris flows (a mixture of sand, clay and water) to high-concentration turbidity currents can occur when the debris flow reaches the standing water and they pointed out that the mode of flow transformation depends on the head velocity of the flow. If the velocity is below the critical threshold, subaerial debris flows make a transition to subaqueous debris flows. In contrast, when the critical value is exceeded, they transform instantaneously into turbidity currents. Naruse and Masuda found that flow transformation occurs only in the head of the flow while the body of a flow remains in a debris flow state.

However, many landslides impacting against a water basin, such as rock-avalanches or debris-avalanches, have more granular rather than cohesive behaviour (Mazzanti 2008). Some dynamic differences between cohesive and granular slides impacting against a water basin may be expected. A granular flow may affect a larger portion of water, as the water in the interstices will be set in motion. Furthermore, in a granular flow the drag against the flow would be expected to be large, as each single grain may be surrounded by water. Whereas the impact of one single intact body is known to be very significant in tsunami generation (Hills and Mader 1997; Harbitz et al. 2006), little is known concerning the collision of a mass composed of a myriad of grains.

To the authors' knowledge, the behaviour of granular, non-cohesive flows impacting against water has been poorly addressed experimentally. In this work a series of experiments were undertaken with artificial small-scale granular flows plunging into a water tank. By using different kinds of materials, it was possible to examine the factors which play a significant role in the dynamics of the experimental flow. In addition to flow transformation, other novel mechanisms have been observed in the experiments and are discussed below.

Experimental setup

The experiments were performed using a 1.2 m long, 0.25 m wide Plexiglas flume, partially immersed in a 0.8 m long, 0.3 m high and 0.6 m wide tank (Fig. 1). Using a pulley, the flume can be inclined from an angle of 10° to a value close to 90°. The tank can be completely filled with water so that the lower end of the flume is immersed to a maximum length of nearly 300 mm. Movies and pictures have been collected by means of two standard digital-video cameras located at the end of the tank (just in front of the flume) and about 1 m above the tank (Fig. 1).

Experiments and results

A total of 30 tests were undertaken using three different types of grains (Table 1), both with an empty tank and after

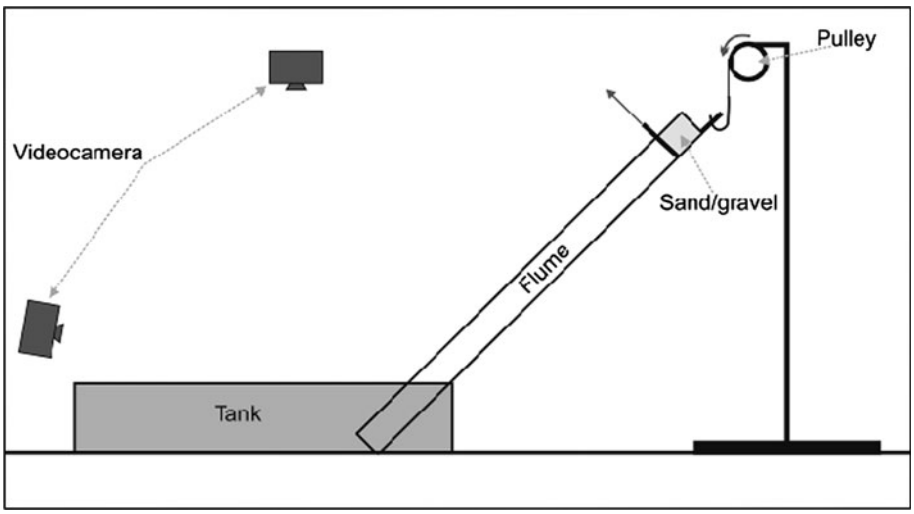

Fig. 1 Sketch showing the experimental setup

Table 1 Properties of grains used in the experiments

	Grain shape	Diameter (mm)	Roundness	Density (g/cm^3)	Rock
A	Fine	0.5–1	Angular	2.65	Quartz
B	Coarse	4–6	Sub-angular	2.6	Syenite
C	Coarse flat	6–80	Angular	2.5	Shale

filling it with water. The angle of inclination of the flume was set to values ranging from 35° to 50° for both wet and dry experiments. Tests with grains A and B were undertaken with and without water in order to examine the main differences between subaerial and subaqueous deposits. Grains C were used only for experiments with water in order to investigate water impact.

Deposit distribution: subaerial versus subaqueous

Figures 2 and 3 show the differences between subaerial and subaqueous deposits recorded using grains A and B, respectively. In the subaerial experiments the shape of the final deposit appears more irregular and blurred at the edges. A lot of grains blanket the base of the tank. These grains moved forward at high speed during the fall and some overshot the tank rim. In contrast, in the subaqueous case, there is much less spreading of the grains; the edges of the deposits are neat. The difference between the subaerial and subaqueous deposits is greater in the case of coarse grains B. The run-out is reduced when the granular flows moved in water rather than in air; this aspect is more evident with fine grains A. These results confirm the importance of the drag forces acting on the granular mass to reduce the run-out of subaqueous landslides. The complete lack of grains moved during the flow suggests that the drag forces are more effective on single blocks and that the

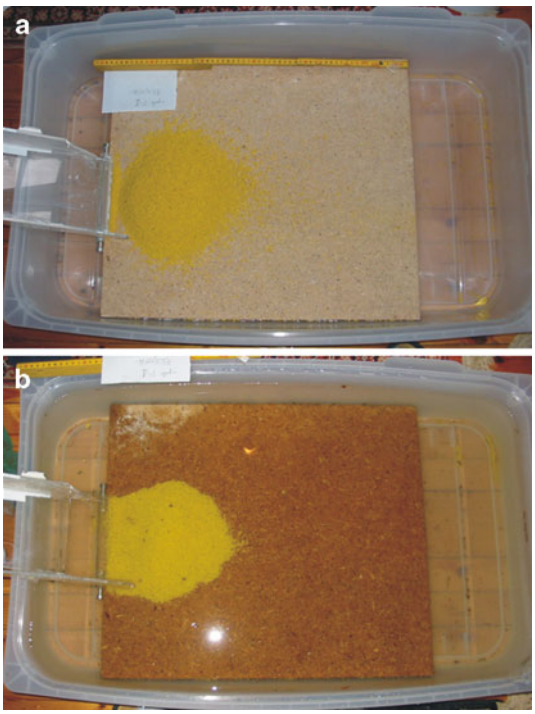

Fig. 2 Final deposit of grains A (Table 1) in the sub-aerial (**a**) and underwater (**b**) experiments

impact forces between grains are significantly reduced in landslides propagating underwater.

Theoretical interpretations and extrapolation to field cases

The velocity of the grains at the base of the flume was estimated as between $\approx$1.3 and 1.5 m/s. Assuming a coefficient of restitution of $\varepsilon \approx 0.7$, the grain bouncing velocity is about $\approx$0.91–1.05 m/s. These velocities imply a maximum horizontal "jump" of about 200 mm. Hence, the

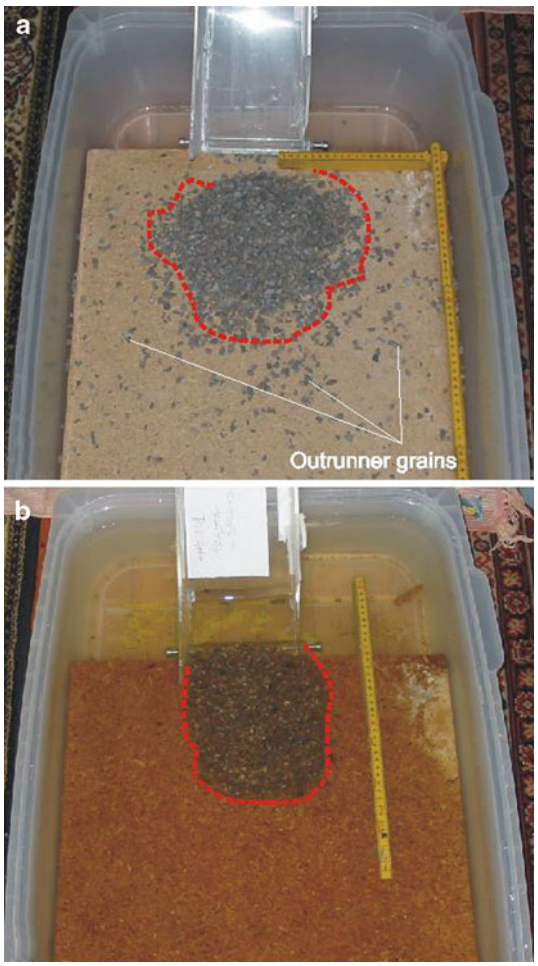

Fig. 3 Final deposit of grains B (Table 1) in the sub-aerial (**a**) and underwater (**b**) experiments. *Dotted red lines* bound the main deposit

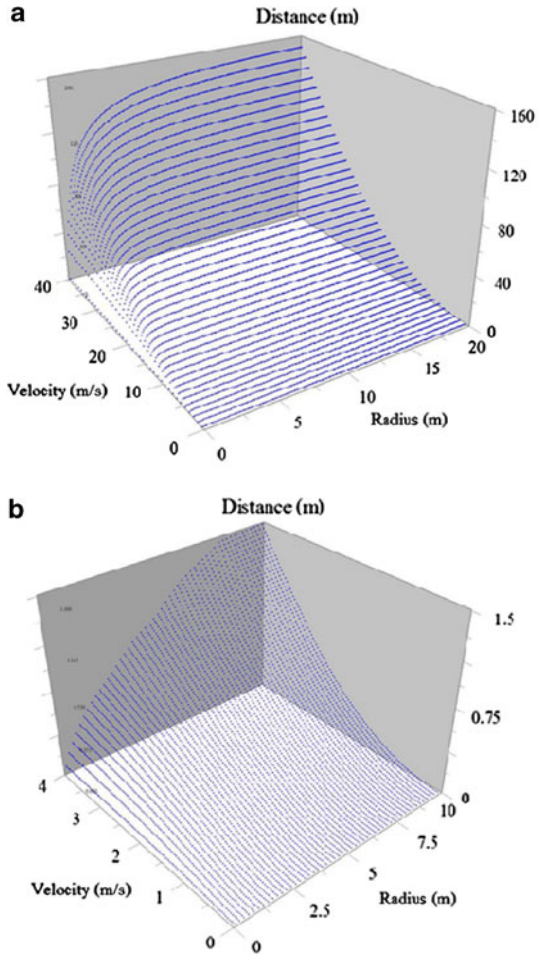

Fig. 4 The horizontal run-out distance in water of a spherical block launched at a given speed. The initial velocity vector has an inclination of 45° from the horizontal. **a** Analysis for large blocks and high initial speed. **b** Centimetre-sized grains at low initial speed

particles at the front of the subaerial granular lobe have bounced out of the main mass. After the first impact, most of these particles were observed to roll to their final location. A similar dynamic could be invoked for the huge velocity (of the order of 100 m/s) reached by blocks in the Nevados Huascaran rock avalanche of 1970 (Plafker and Eriksen 1978).

It is considered that the additional drag force may explain the lack of particle spread in the corresponding subaqueous experiments. Assuming the same initial velocity as for the subaerial case and restricting the analysis to fine particles "A", the particle Reynolds number can be estimated as

$$Re_p = \frac{\rho_w u D}{\mu} \approx 0.7 \times 10^3 \tag{1}$$

which corresponds to a drag coefficient of $C_D \approx 4.0$ for a non-spherical grain of roundness $\psi = 0.6$ and $C_D \approx 0.5$ for $\psi = 1$ which corresponds to perfectly spherical grains (Rhodes 1998). The initial deceleration in water for the $\psi = 0.6$ grain is about

$$g' \equiv \frac{dv}{dt} = -\frac{1}{2}\rho_w u^2 C_D \times \frac{\text{particle cross surface}}{\text{particle mass}} = -\frac{3}{8} C_D \frac{\rho_w}{\rho} \frac{u^2}{R} \approx -15g \tag{2}$$

expressed in terms of the gravity acceleration g, whereas for the spherical grain $g' \approx -1.8\ g$. A stopping distance can be estimated assuming constant deceleration as

$$s = \frac{u^2}{2g'}, \tag{3}$$

This was found to be in the order of millimetres and centimetres for non-spherical and spherical grains, respectively. The deceleration values decrease considerably as the particle reduces its speed.

To study the distance reached by spherical particles moving in water, the trajectory of one particle with an

initial speed v_0 and velocity vector inclined at 45° to the horizontal was considered. The dependence of the drag coefficient on the Reynolds number is assumed as a fit to the drag curves reported, for example, by Rhodes (1998)

$$\begin{array}{ll} C_D = 24/Re + 0.44 & \text{if} \quad Re < 2 \times 10^5 \\ 0.1 & \text{if} \quad Re > 4 \times 10^5 \end{array}$$

with a linear interpolation when $2 \times 10^5 < Re < 4 \times 10^5$.

Figure 4 shows the results for the small-scale case (A) and the large-scale case (B). For the case of yellow grains (particle radius of 0.2 mm and speed 1 m/s) the calculation predicts a distance of about 20 mm, which is consistent with the lack of dispersed grains. For the coarse grains "B", the maximum distance is about 50 mm. To deal with a more realistic sphericity index of 0.6, the fit of the drag coefficient was changed to the values provided by Rhodes (1998), which gave distances of 3 and 10 mm, respectively. Note that in air the drag force for this particle size and velocity range represents a very small correction. Larger grains and higher velocities can give a far greater distance as shown in the figure. The prediction for the large-scale case (B) shows that the distance reached by a boulder with initially high speed may be quite considerable. For example, a 20 m radius boulder travelling at a speed of 40 m/s will reach a distance of about 160 m.

Nevertheless, in subaqueous landslides boulders and blocks scattered around the foot of submarine landslides are sometimes found several kilometres from the main landslide body (Prior et al. 1984; Kuijpers et al. 2001; Longva et al. 2003; De Blasio et al. 2006) despite the very gentle slopes. The above calculations show that boulders in ballistic flight in water are not capable of reaching long distances, hence other mechanisms must be invoked to explain the presence of blocks several kilometres far from the main debris flow deposit (De Blasio et al. 2006; Mazzanti and De Blasio 2009).

Air ejection

Experimental observations

The experiments performed with coarse grains in subaqueous conditions revealed the presence of several bubbles around and over the moving mass once it plunges and propagates underwater. Two different types of bubbles have been recognized which are produced in the early and final stage of the underwater path respectively.

The bubbles produced in the early stage (Figs. 5, 6a) are very large in comparison with the grain size and arise as the granular mass enters the water. These bubbles are produced by the air-cavitation (Knapp et al. 1970; Plesset and Prosperetti 1977), a well known phenomenon for high speed objects diving in water like projectiles (Lee et al. 1997; Hong-Hui et al. 2000), missiles (May 1952) and landslides (Fritz et al. 2003). This effect is also considered very important for the tsunamigenic potential of subaerial masses plunging into water (Fritz et al. 2003).

The bubbles which rise in the final stage of the mass-flow (Figs. 5, 6b) are completely different from the air-cavity bubbles, being significantly smaller in size and more numerous. The similarity in size between the grains and final stage bubbles suggests a different origin from the initial stage bubbles and they may arise from the leakage of the air trapped inside the mass during the subaerial movement. This effect would occur in the final stage of the flow as the internal earth pressure (Savage and Hutter 1989) of the mass changes from the passive to the active state. Similar phenomena have been documented in large subaerial rock avalanches and have been described as "Pavoni tubes" (Pavoni 1968; Poschinger and Haas 1997). In the main landslide debris, they are characterized by vertically oriented tubes where fine grains are completely absent; Pavoni interpreted this feature as the result of the leakage of the water or air from the base of the moving mass, carrying with it the finer portion of the sediments.

Theoretical interpretation

As a simple model for the ejection of air from the submerged granular matrix an artificial granular avalanche of a permeable homogeneous material was considered. For simplicity the granular medium was arranged in a circular plate of thickness L and radius $W \gg L$. As a consequence of the chosen geometry, the water flows inside the avalanche, perpendicular to the top and bottom surfaces of the plate, whereas the flow from the sides is negligible (see Fig. 7).

The water flux is given as

$$v = \frac{k}{\mu}\frac{\partial P}{\partial y} \tag{4}$$

where μ is the water viscosity and y is the direction perpendicular to the plate faces (Fig. 7). Considering that water pressure is $P = \rho g D$, where D is the depth, the time needed for water to fill the whole medium is about

$$\tau \approx \frac{L}{v} = \frac{\mu L^2}{kgD\rho} \tag{5}$$

Representative values for the permeability were taken as 10^{-5} cm^2 $= 10^{-9}$ m^2 for coarse sand and 10^{-6}–10^{-8} cm^2 $= 10^{-10}$–10^{-12} m^2 for very fine sand. For $L = 0.05$ m and $D = 0.1$ m, in the order of 1 s and $\gg$10 s was required for coarse and fine sand respectively before the air is liberated. However, in these estimates it is

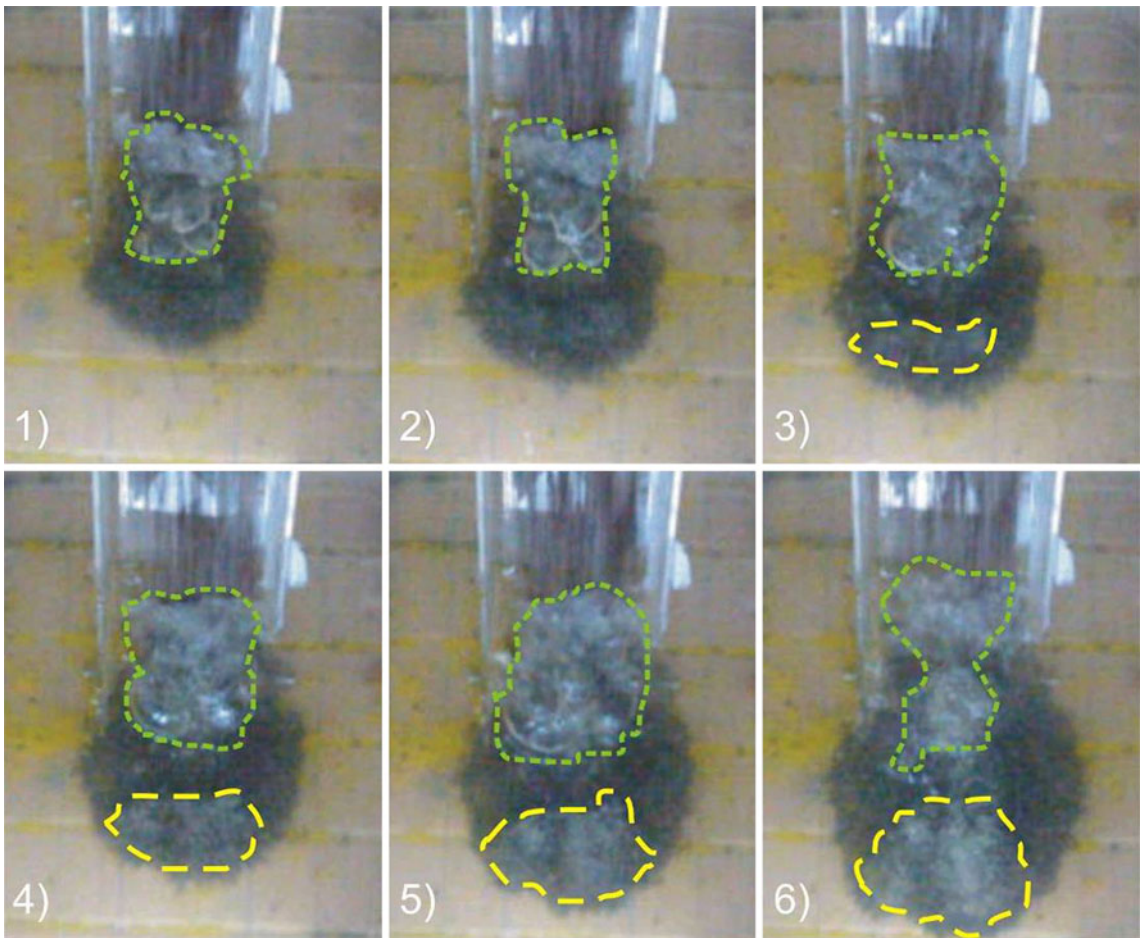

Fig. 5 Six consecutive frames corresponding to about 1 s of the final deposition in the subaqueous case, using grains B. *Dotted green lines* bound large bubbles due to air cavitation; *dashed yellow lines* bound small bubbles due to air ejection

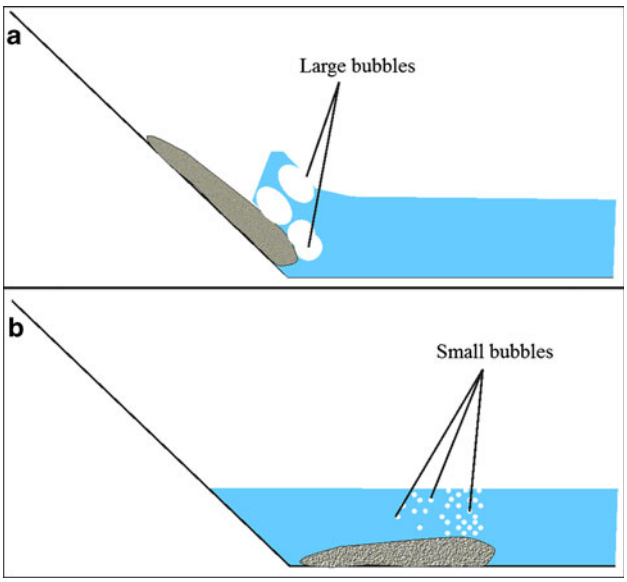

Fig. 6 Sketch of the two types of bubbles shown in Fig. 5. **a** Large bubbles due to air in a cavity; **b** small bubbles caused by air ejection

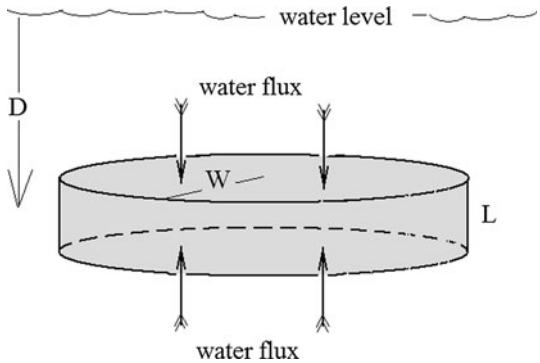

Fig. 7 Explanation of the geometry for the calculation of the time needed for water to fill a disk of granular medium at depth D

assumed that the granular medium maintains the same solid density. In practice, a solid density of a deforming landslide will decrease, thus the permeability is substantially increased and the time for the water to penetrate the medium is reduced.

Applications to field studies

The time needed for water penetration (or air liberation) is

$$\frac{\tau_{\text{field}}}{\tau_{\text{lab}}} = \left(\frac{L_{\text{field}}}{L_{\text{lab}}}\right)^2 \left(\frac{D_{\text{lab}}}{D_{\text{field}}}\right)\left(\frac{k_{\text{lab}}}{k_{\text{field}}}\right) \quad (6)$$

If for simplicity it is assumed that D increases linearly with L, the liberation time becomes proportional to the thickness of the slide. Assuming a scaling factor of 100 between the laboratory and the field and the same value for the permeability as used in the laboratory experiments, typical residence times for air in the body of the slide range between 0.25 and 250 s.

In natural landslides the presence of trapped air can significantly affect the dynamic behaviour by producing density reduction of the whole mass and a non-negligible increase of the buoyancy forces. The effective gravity acceleration g' (taking account of the buoyancy term) becomes

$$g' = 1 - \frac{\rho_W}{\rho(1-\varepsilon)}g \quad (7)$$

where ε is the void fraction in the granular medium. The reduction factor can be very significant especially for low density media, with some 20–30% reduction of the effective gravity field with typical values $\varepsilon \approx 0.3$.

The result of facilitating the buoyancy is a prolonged floating at shallower depths. This may have three important consequences on the dynamics of the landslide.

(a) An extended impact time with the surface of the water may enhance the tsunami generated by a granular landslide.
(b) The prolonged lack of contact between the slide and the sea bottom results in reduced friction and improved mobility.
(c) Finally, the possible presence of a sack of air trapped between the base of the flowing mass and the sliding plane could act as a lubricant, amplifying the slide mobility.

Air to water transition

The transition phase between air and water in a coastal landslide must be considered as the main distinctive feature between completely subaerial and completely subaqueous gravity flows. Since the early work of von Karman (1929), various studies have been carried out on objects with a simple shape, e.g. spheres, disks etc., with the aim of investigating this transition, which significantly affects both the moving mass and the water table. The experiments show the complex mechanisms related to the transition, mainly in terms of air cavitation (Plesset and Prosperetti 1977; Lee et al. 1997) and shock on the impacting body (Fasanella et al. 2003). Some papers have been concerned with the interaction of pyroclastic flows with the sea, using both theoretical analyses and/or laboratory experiments (Freundt 2003; Legros and Druitt 1999) as well as real cases such as the 1883 Krakatau eruption (Carey et al. 1996). However, little investigation has been dedicated to the transition in coastal landslides, although clearly it could play an important role in the evolution of fast gravity flows (Mazzanti 2008).

In the present study, particular attention has been devoted to the investigation of this transition phase. The effects of the impact on the moving mass was limited in the experiments performed using coarse grains (apart from a limited thickening of the head of the mass), while it was quite evident with the fine grains (A). In this case a sudden reduction in velocity upon impact resulted in the rising of

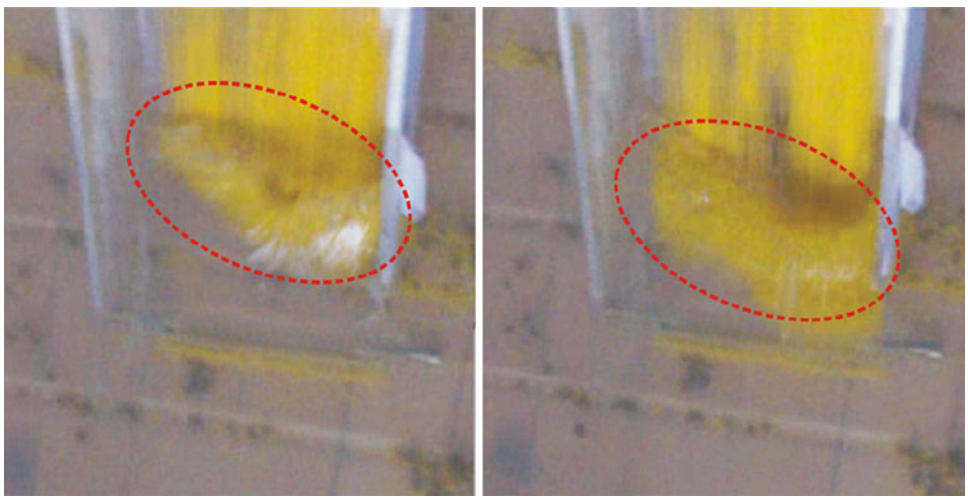

Fig. 8 Two consecutive frames showing the early stages of water impact, using grains B

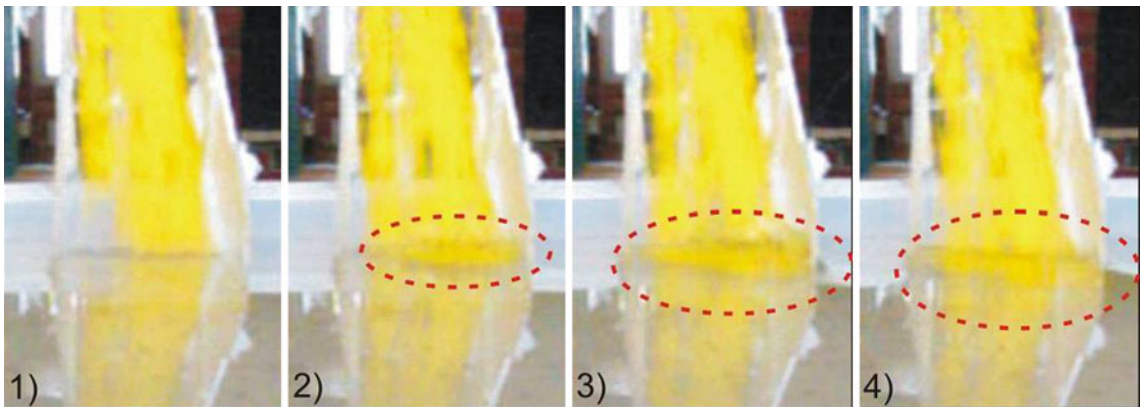

Fig. 9 Frames showing a frontal view of water impact using grains B. *Dashed red* ellipses enclose the particles floating over the water surface

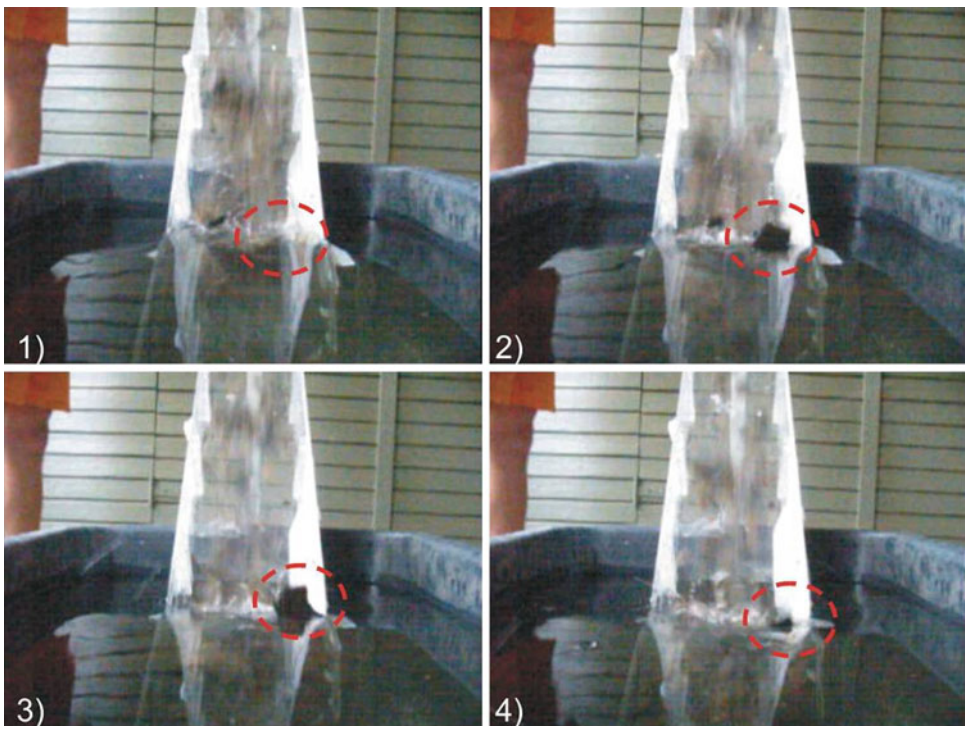

Fig. 10 Frames showing a frontal view of water impact using grains C. The *dashed red circles* enclose one particle affected by tilting at the water surface

the grain and a consequential thickening of the frontal part of the flow, with some floating of particles in the original mass (Fig. 8). As can be seen in Fig. 9, over time there is a significant increase of the area affected by floating such that, following the impact, a portion of the mass is "surfing" at water level. The process of "surfing" has been suggested as a theoretical possibility and observed in some real landslides (Ter-Stepanian 2002; Mazzanti 2008; Chen and Hawkins 2009; Mazzanti and De Blasio in preparation).

Flat grains C (Table 1) were used to examine this effect. As can be seen from Fig. 10, surfing was observed in the early stage of impact with spectacular effects such as "tilting" (Fig. 10) and "jumping" (Fig. 11) of single particles; indeed, some of the particles were capable of jumping nearly 2 m ahead of the impact point. Particles that did not jump were seen to float into the water tank at high speed, exhibiting peculiar patterns of floating and whirling, and again sometimes travelling long distances. The different types of water impact are shown schematically in Fig. 12.

To further examine these mechanisms, different angles of inclination of the flume and different velocities of the mass were used; higher velocities were obtained by prolonging the flume length by 800 mm to 2 m. The results show that the most notable surfing effects were achieved

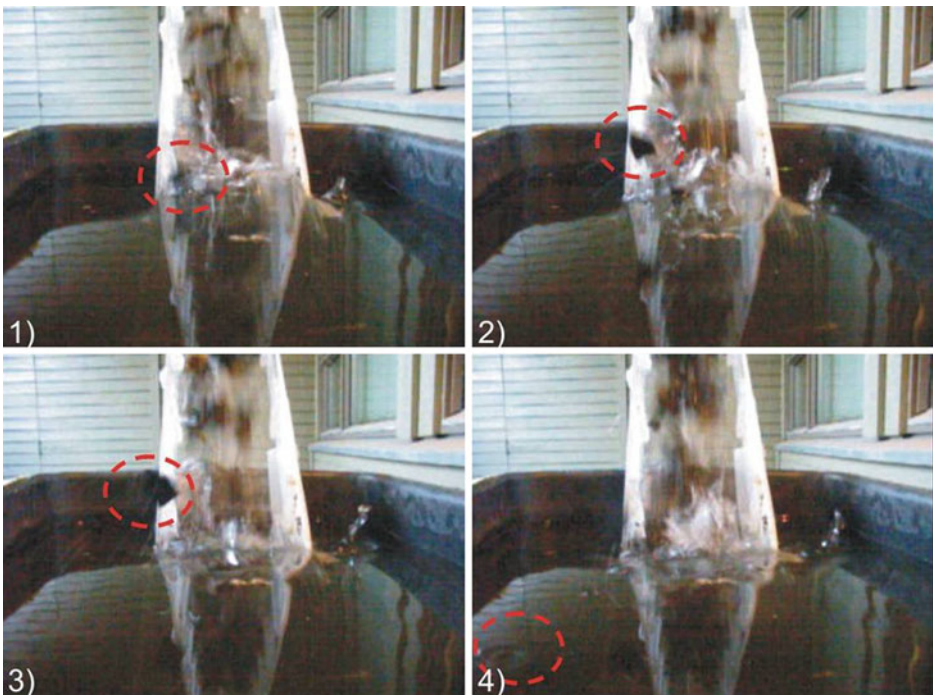

Fig. 11 Frames showing a frontal view of water impact using grains C. The *dashed red circles* enclose one particle affected by jumping at the water surface

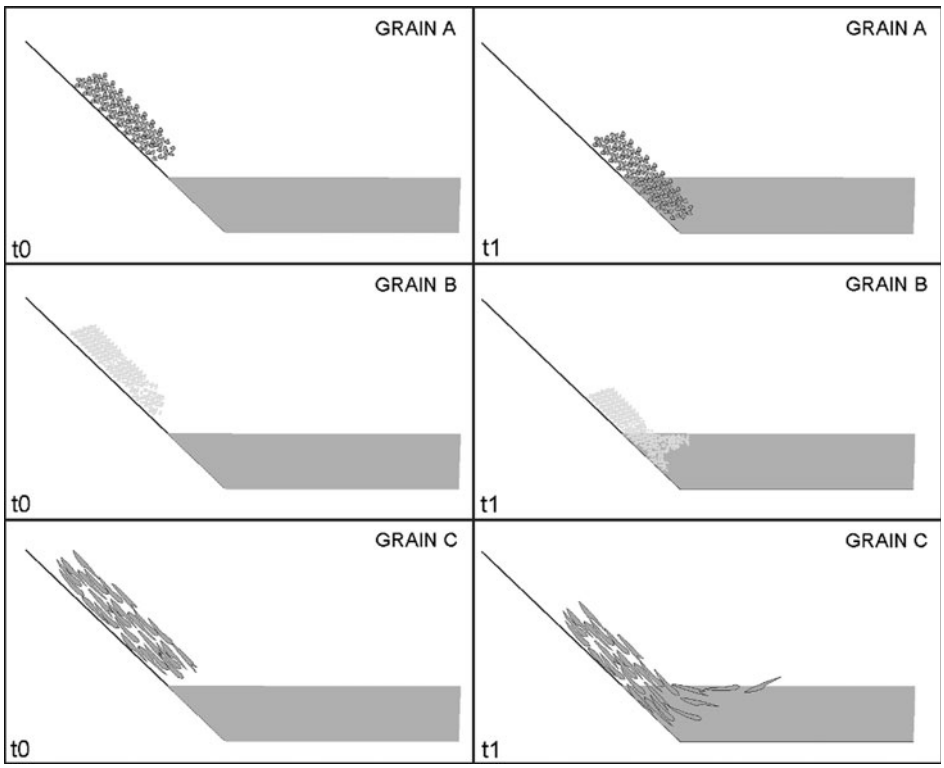

Fig. 12 Sketch describing the three different types of water impact using *grains A*, *B* and *C*

with high velocity and small angle of inclination. Tilting/surfing of single grains and thickening at the front occurred for fine and coarse flat grains, respectively; in these cases, the effects were recorded independent of the geometry and velocity of impact. In contrast, no significant effects were recorded using coarse round grains.

It is suggested that the interaction between the mass and the water surface is largely controlled by the features of the flowing mass although different parameters (e.g. grain size and shape, angle of inclination between the flume and the water surface and/or velocity of impact) can lead to different mechanisms such as surfing, tilting and flip-back of single flat particles.

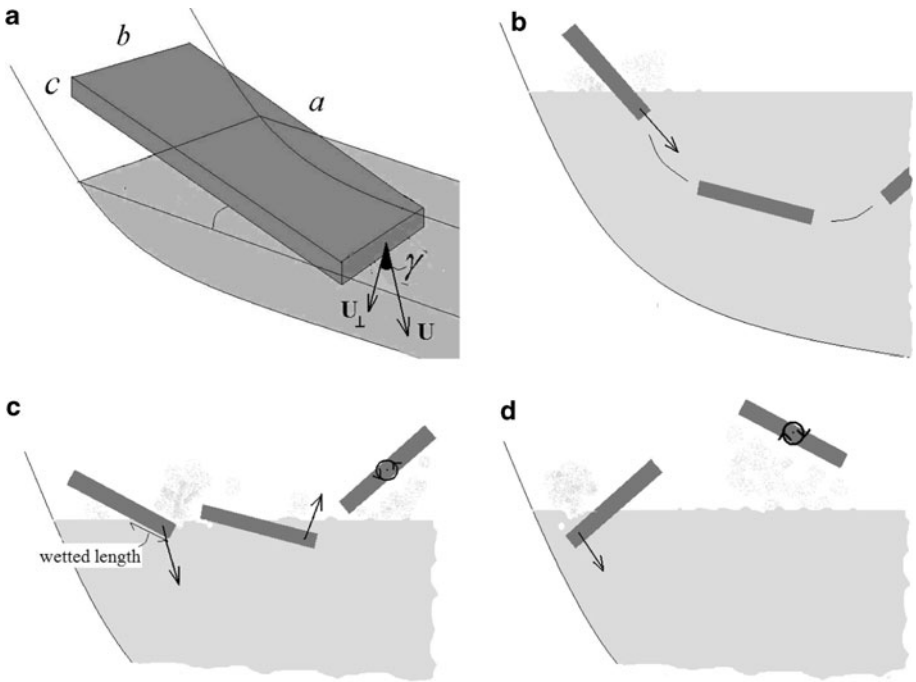

Fig. 13 Geometry of a slab impact against the water surface. **a** Basic geometric definitions. **b** Head-on impact where the velocity vector is parallel to the surface of the largest block. **c** Head impact: the block bounces against the surface and starts rotating anticlockwise. **d** Tail impact: the block starts rotating clockwise

Similar phenomena have been induced by geomorphological features and have been recorded by videos of real events (Mazzanti 2008).

Impact: theoretical estimates

The model used a parallelepiped block with the longest axis (a) parallel to the direction of movement; b is the dimension perpendicular to the direction of movement, and c is the block thickness (Fig. 13a).

A block entering the water approximately parallel to its main face (Fig. 13a) will plunge in at high speed. The flatness of the block gives a hydrodynamic shape and low drag as the skin friction coefficient (i.e., the resistance acting on the lateral faces of the block) is very low compared with the front drag, which is limited by the size of the front area (Schlichting 1962). As a consequence, the flat block maintains a high speed for a prolonged time and as it builds up a curvilinear path beneath the water surface, it may eventually reach the water surface again.

If the block hits the water surface skewed as in Fig. 13c, the torque and the force on the centre of mass increase enormously compared to a head-on impact. The block may suddenly change its direction of motion and reduce in speed; at the same time the torque will begin to rotate. Alternatively, the back of the block may hit the water first (Fig. 13d), such that the block starts to spin clockwise (with reference to the figure). The last two cases correspond to the bouncing observed experimentally.

The estimates developed here are meant to capture the general behaviour by an order of magnitude, without pretence of a detailed description. A more comprehensive theoretical analysis will be the subject of a future paper.

When hitting the water surface with its front end, the block experiences an instantaneous torque of the order

$$T \approx \frac{1}{4}\rho_W U_\perp^2 (\lambda - \lambda^2) a^2 b \tag{8}$$

where λa is the wetted length, i.e. the length of the block in contact with water (Fig. 13c) and $U_\perp = U \sin\gamma$ is the velocity component perpendicular to the main plane of the block, with γ the angle between the velocity of the front and the axis perpendicular to that plane. Equating this quantity to $I\dot{\Omega}$, where $\dot{\Omega}$ is the rate of change of angular velocity and I is the moment of inertia of the parallelepiped around the axis b passing through the centre,

$$\dot{\Omega} \approx \frac{U_\perp^2 (\lambda - \lambda^2)}{2ac} \frac{\rho_W}{\rho} \tag{9}$$

hence, the angular acceleration depends critically on the direction of velocity at the instant of impact with the water surface. In turn, the velocity depends on the geometry of the flume, on the grain shape and also poorly controllable elements such as the velocity component perpendicular to the flume at the tip of the block. In view of the velocity fluctuations, it is reasonable to expect that for some blocks $U_\perp$ will be a large proportion of the velocity U.

To fix a representative value, it was assumed that the maximum value attained by $U_\perp$ is $\approx U/\sqrt{2}$, so that the

velocities of the block front perpendicular and parallel to the main face are the same. As soon as the block starts rotating, the angle of impact changes. To calculate the orientation of the block as a function of time, it is necessary to integrate the equation of motion for the centre of mass of the block and for its spinning angle. For typical experimental values ($a \approx 0.2$ m; $c \approx 0.01$ m; $U \approx 1$ m/s) it was found that $\dot{\Omega} \approx 60\ \mathrm{s}^{-2}$, a very large value for the angular acceleration. The time needed for a 90° flip is of the order $\tau \approx \left(\pi/\dot{\Omega}\right)^{1/2} \approx 0.2$ s, which explains the very rapid flip-back of particles observed experimentally. For a natural landslide block, $a \approx 10$ m; $c \approx 1$ m; $U \approx 30$ m/s were considered reasonable. This gives $\dot{\Omega} \approx 11\ \mathrm{s}^{-2}$, a realistic value. The time needed for a 90° flip in this case would be about half a second. However, it is also possible that a block subjected to such a very large torque would break upon impact with the water surface.

Conclusions

The dynamics of coastal landslides starting in a subaerial setting and plunging into water were investigated through laboratory experiments using granular material. In spite of their simplicity, the experiments offer some interesting insights into the mechanisms that characterize the propagation of coastal landslides.

1. Different features in terms of the final deposit for the subaerial and the subaqueous cases have been recognized. In contrast to purely subaerial flows, underwater flows do not produce "outrunner grains" and thus, the final deposit is more compact. Moreover, the run-out distance is significantly lower due to the drag forces exerted by the water on the moving mass. This evidence is consistent with theoretical works suggesting a strong reduction in grain to grain impact and an increase in the resistant forces in water (Mazzanti 2008).
2. These experiments indicated a leakage of pore air from the body during the final part of the mass movement. A significant amount of air could be trapped inside the granular mass during its aerial path, which is then released when the mass comes to rest and the inner earth pressure changes from the passive to the active state. This effect results in a modification of the dynamic behaviour of the granular mass, with a decrease in the bulk density and a subsequent increase in the buoyancy force during the subaqueous path. Simple physical analyses show that such trapping of air may also take place in natural landslides, thus modifying their dynamic behaviour. An obvious consequence is the prolonged lack of contact between the sliding mass and the terrain, which favours the landslide mobility.
3. The air to water transition is the most critical phase due to the strong and sudden forces exerted by the water surface, which may lead to sudden changes in the landslide dynamics. To elucidate the physical effects upon impact, both flat and rounded blocks were used in the experiments. The results indicated that the interaction between the mass and the water surface is largely determined by: (a) the features of the flowing mass (size and shape of the grains), (b) the angle of inclination between the flume and the water surface and (c) the impact velocity. With rounded grains the mass experienced a rising and thickening of the frontal part of the flow; otherwise, with small grains the mass travelled over the water surface.
4. Using flat grains, under favourable conditions (i.e. high velocity, low angle between the flume and the water surface), the impact force combined with the rigidity of the blocks resulted in them being propelled into the air on impact. Simple physical estimates indicate that the same phenomena may occur in natural coastal landslides and significantly affect their dynamics.
5. The effects observed may also influence the characteristics of tsunami, increasing or decreasing the induced wave height and distribution. In spite of the rapid development and the scientific efforts carried out in the last years, there are still large gaps in the understanding of tsunamis induced by subaerial landslides. More detailed investigations should be carried out in order to understand the main mechanisms which rule the transition phase.

In spite of their simplicity, the experiments presented in this paper have demonstrated several unusual phenomena which may also occur in real flow-like granular coastal landslides. The work has shown that combined subaerial–subaqueous mass movements involve phenomena distinctive of both kinds of landslides, as well as a transition phase, which can be very complex.

References

Breien H, Pagliardi M, De Blasio FV, Issler D, Elverhøi A (2007) Experimental studies of subaqueous vs. subaerial debris flows—velocity characteristics as a function of the ambient fluid. In: Lykousis V, Sakellariou D, Locat J (eds) Submarine mass movements and their consequence, pp 101–110

Carey S, Sigurdsson H, Mandeville C, Bronto S (1996) Pyroclastic flows and surges over water: an example from the 1883 Krakatau eruption. Bull Volcanol 57:493–511

Chen H, Hawkins AB (2009) Relationship between earthquake disturbance, tropical rainstorms and debris movement: an overview from Taiwan. Bull Eng Geol Environ 68:161–186

De Blasio FV, Engvik LE, Elverhøi A (2006) Sliding of outrunner blocks from submarine landslides. Geophys Res Lett 33:L06614. doi:10.1029/2005GL025165

Fasanella EL, Jackson KE, Sparks CE, Sareen AK (2003) Water impact test and simulation of a composite energy absorbing fuselage section. J Am Helicopter Soc 50(2):150–164

Felix M, Peakall J (2006) Transformation of debris flows into turbidity currents: mechanisms inferred from laboratory experiments. Sedimentology 53:107–123

Freundt A (2003) Entrance of hot pyroclastic flows into the sea: experimental observations. Bull Volcanol 65:144–164

Fritz HM, Hager WH, Minor HE (2003) Landslide generated impulse waves. 2. Hydrodynamic impact craters. Exp Fluids 35:520–532

Hampton MA (1972) The role of subaqueous debris flows in generating turbidity currents. J Sed Petrol 42:775–793

Harbitz CB, Løvholt F, Pedersen G, Masson DG (2006) Mechanisms of tsunami generation by submarine landslides: a short review. Norwegian J Geol 86:255–264

Hills JG, Mader CL (1997) Tsunami produced by the impact of small asteroids. Ann N Y Acad Sci 882:381–394

Hong-Hui S, Motoyuki I, Takuya T (2000) Optical observation of the supercavitation induced by high-speed water entry. J Fluid Eng 122:806–810

Ilstad T, Elverhøi A, Issler D, Marr J (2004) Subaqueous debris flow behaviour and its dependence on the sand/clay ratio: a laboratory study using particle tracking. Mar Geol 213:415–438

Iverson RM (1997) The physics of debris flows. Rev Geophys Res 35:245–296

Iverson RM, Costa JE, LaHusen RG (1992) Debris flow flume at H. J. Andrews Experimental Forest, Oregon, US. Geol Surv Open File Rep 92–483:2

Knapp RT, Daily JW, Hammitt FG (1970) Cavitation. McGraw-Hill, New York

Kuenen PHH, Migliorini CI (1950) Turbidity currents as a cause of graded bedding. J Geol 58:91–107

Kuijpers A, Nielsen T, Akhmetzhanov A, De Haas H, Kenyon NH, van Weering TCE (2001) Late Quaternary slope instability on the Faeroe margin: mass flow features and timing of events. GeoMar Lett 20:149–159

Lee M, Longoria RG, Wilson DE (1997) Cavity dynamics in high-speed water entry. Phys Fluids 9:540–550

Legros F, Druitt TH (1999) On the emplacement of ignimbrite in shallow-marine environments. J Volcanol Geother Res 95:9–22

Longva O, Janbu N, Blikra LH, Bøe R (2003) The 1996 Finneidfjord slide; seafloor failure and slide dynamics. In: Submarine mass movements and their consequences. Springer, New York, pp 531–538

Marr JG, Harff PA, Shanmugam G, Parker G (2001) Experiments on subaqueous sandy gravity flows: the role of clay and water content in flow dynamics and depositional structures. Geol Soc Am Bull 113(11):1377–1386

May A (1952) Vertical entry of missiles into water. J Appl Phys 23:1362–1372

Mazzanti P (2008) Analysis and modelling of coastal landslides and induced tsunamis. PhD Thesis, University of Rome "Sapienza", 214 pp

Mazzanti P, De Blasio FV (2009) Peculiar morphologies of coastal and subaqueous landslides deposits and their relationship to flow dynamics. In: Mosher DC, Shipp C, Moscardelli L, Chaytor J, Baxter C, Lee H, Urgeles R (eds) Submarine mass movements and their consequences IV; Advances in natural and technological hazards research, Vol 28. Springer, The Netherlands, pp 141–151

Mohrig D, Elverhøi A, Parker G (1999) Experiments on the relative mobility of muddy subaqueous and subaerial debris flows, and their capacity to remobilize antecedent deposits. Mar Geol 154:117–129

Pavoni N (1968) Uber die Enstehung der Kiesenmassen im Bersturzgebiet von Bonaduz-Reichenau (Graubunden). Eclogae Geol Helv 61:494–500

Plafker G, Eriksen GE (1978) Nevados Huascaran Avalanches, Peru. In: Voight B (eds) Rockslides and avalanches, vol 1. Elsevier, Amsterdam, pp 48–55

Plesset MS, Prosperetti A (1977) Bubble dynamics and cavitation. Ann Rev Fluid Mech 9:145–185

Poschinger A, Haas U (1997) Der Flimser Bergsturz, doch ein warmzeitliches Ereignis?, Bull. Angew Geol 2:35–46

Prior DB, Borhold BD, Johns MW (1984) Depositional characteristics of a submarine debris flow. J Geol 92:707–727

Pudasaini SP, Hutter K (2007) Avalanche dynamics. Springer, Heidelberg

Rhodes M (1998) Introduction to particle technology. Wiley, Chichester

Savage SB, Hutter K (1989) The motion of a finite mass of granular material down a rough incline. J Fluid Mech 199:177–215

Schlichting H (1962) Boundary layer theory, 4th edn. McGraw-Hill, USA

Talling PJ, Peakall J, Sparks RS, Cofaigh CO, Dowdeswell JA, Felix M, Wynn RB, Baas JH, Hogg AJ, Masson DG, Taylor J, Weaver PPE (2002) Experimental constraints on shear mixing rates and processes: implications for the dilution of submarine debris flows. In: Dowdeswell JA, Cofaigh CÓ (eds) Glacier-influenced sedimentation on high-latitude continental margins. Geological Society of London, Special Publication 203:89–103

Ter-Stepanian G (2002) Suspension force and mechanism of debris flows. Bull Eng Geol Environ 61:197–205

von Karman T (1929) The impact of sea planes floats during landing. NACA TN, 321